Electronic Supplementary Material (ESI) for Energy & Environmental Science

Supporting Information for

Analysis of the Operation of Thin Nanowire Photoelectrodes for Solar Energy Conversion

Justin Foley,[1*] Michelle J. Price,[1*] Jeremy Feldblyum,[2] and Stephen Maldonado[1,3]**

1) Program in Applied Physics
2) Macromolecular Engineering
3) Department of Chemistry
930 N University
Ann Arbor, Michigan 48109-1055

* These authors contributed equally to the preparation of this work
** To whom correspondence should be addressed. Phone: 734-647-4750.
E-mail: smald@umich.edu Home Page: http://www.umich.edu/~mgroup/

Electronic Supplementary Material (ESI) for Energy & Environmental Science

S1. Overview

This document contains derivations of the current density formulas for the bulk recombination and depletion region recombination limits in sections S2 and S3. In Section S4, a description of the device grid used in the simulations is presented. In Section S5, a set of tables listing the parameters used in each simulation dataset discussed in the main text are collected. A listing of the references cited within this document is included on the final page in Section S6.

S2. Expression for Bulk Recombination Current Density in an Infinite Cylindrical Photoelectrode

For an n-type semiconductor photoelectrode in the dark at equilibrium, the minority carrier current, J_p, is given by eq S1,

$$\frac{\partial p}{\partial t} = 0 = -U_p + \frac{1}{q}\nabla \cdot J_p \tag{S1}$$

where the recombination rate in the bulk, $U(r)$ is given by eq S2

$$U(r) = \frac{p(r) - p_0}{\tau_p} \tag{S2}$$

In cylindrical coordinates, assuming the radial dimension, r, is much shorter than the length of the nanowire and that carrier diffusion is the only process controlling J_p, eq S2 can be expressed as eq S3.

$$\frac{p(r) - p_0}{\tau_p} = D\nabla^2 p(r) = D\frac{1}{r}\frac{\partial}{\partial r}\left(r\frac{\partial p(r)}{\partial r}\right) \tag{S3}$$

Eq S3 can be expressed in a more useful form through eqs S4 and S5.

$$\frac{p(r) - p_0}{\tau_p} = D\frac{1}{r}\left(\frac{\partial p(r)}{\partial r} + r\frac{\partial^2 p(r)}{\partial r^2}\right) \tag{S4}$$

$$\frac{\partial^2 p(r)}{\partial r^2} + \frac{1}{r}\frac{\partial p(r)}{\partial r} - \frac{p(r) - p_0}{D\tau_p} = 0 \tag{S5}$$

Eq S5 is Bessel's differential function, where $p(r)$ can be expressed in terms of a linear combination of a Bessel function of the first kind, B_0, and a Bessel function of the second kind, Y_0, with constants C_1 and C_2 (eq S6).[1]

$$p(r) - p_0 = C_1 B_0\left(\frac{r}{\sqrt{D_p\tau_p}}\right) + C_2 Y_0\left(\frac{r}{\sqrt{D_p\tau_p}}\right) \tag{S6}$$

Since $(D_p\tau_p)^{1/2} = L_p$, eq S6 can be re-stated as eq S7.

$$p(r) - p_0 = C_1 B_0\left(\frac{r}{L_p}\right) + C_2 Y_0\left(\frac{r}{L_p}\right) \tag{S7}$$

The first boundary condition for $p(r)$ is that $p(r)$ is a finite number at all values of r. (For an infinitely thick nanowire, this boundary condition would become $p(0) = p_0$ in analogy to the boundary condition for a semi-infinite slab) Application of this boundary condition results in eq S8.

$$p(r) - p_0 = C_1 B_0\left(\frac{r}{L_p}\right) \tag{S8}$$

The second boundary condition is given as eq S9, i.e. the Boltzmann distribution of carriers within the semiconductor. This boundary condition is a corollary of flat quasi-Fermi levels throughout the depletion region.

$$p(w) = p_0 e^{\frac{qV}{k_B T}} \tag{S9}$$

Applying the second boundary condition and solving for C_1 yields eq S10.

$$C_1 = \frac{p_0\left(e^{\frac{qV}{k_B T}} - 1\right)}{B_0\left(\frac{w}{L_p}\right)} \tag{S10}$$

Hence, the full expression for $p(r)$ is given by eq S11.

$$p(r) = p_0 + p_0\left(e^{\frac{qV}{k_B T}} - 1\right)\frac{B_0\left(\frac{r}{L_p}\right)}{B_0\left(\frac{w}{L_p}\right)} \tag{S11}$$

The total bulk recombination current is given by the sum of the fluxes of electrons and holes. In an n-type semiconductor, the electron flux at w is zero. Hence, the total bulk recombination current at $r = w$ is given by eq S12.

$$J_{br} = J_{br,n} - J_{br,p} = -J_{br,p} \tag{S12}$$

By definition, $J_{br,p}$ is equal to the gradient of $p(r)$.

$$J_{br,p} = -qD_p \nabla p(r) \tag{S13}$$

Solving eq S13 in a cylindrical coordinate system and evaluating at $r = w$ yields

$$J_{br} = \frac{qD_p p_0}{L_p}\left(\left(e^{\frac{qV}{k_B T}} - 1\right)\frac{B_1\left(\frac{w}{L_p}\right)}{B_0\left(\frac{w}{L_p}\right)}\right) \tag{S14}$$

When $w << L_p$, the limit of the ratio of the Bessel functions is $w/4L_p$. J_{br} can then be written as

$$J_{br} = \frac{qD_p p_0 w}{4L_p^2}\left(e^{\frac{qV}{k_B T}} - 1\right) \tag{S15}$$

Since $n_0 p_0 = n_i^2$ and $n_0 \approx N_D$, eq S16 is a convenient form of the final result.

$$J_{br,cyl} = \frac{qD_p n_i^2 w}{4N_D L_p^2}\left(e^{\frac{qV}{k_B T}} - 1\right) \tag{S16}$$

S3. Expression for Depletion Region Recombination Current Density in an Infinite Cylindrical Photoelectrode

At steady state and under conditions where depletion region recombination is the limiting process, the total recombination rate, $U(r)$, is proportional to the divergence of the recombination current, $J_{dr,cyl}$.

$$U(r) = \frac{1}{q}\nabla \cdot J_{dr,cyl} \tag{S18}$$

In a cylindrical coordinate system where the radial dimension is much less than the length of the nanowire, eq S18 can be explicitly solved for $J_{dr,cyl}$ by integrating over the entire depletion width (i.e. $r_0 - w$).

$$J_{dr,cyl} = q\frac{1}{r}\int_{w}^{r_0} rU(r)dr \tag{S19}$$

The integral term in eq S19 can be rewritten through integration by parts,

$$q\frac{1}{r}\int_{w}^{r_0} rU(r)dr = q\int_{w}^{r_0} U(r)dr - \frac{q}{r}\int_{w}^{r_0}\left(\int U(r)dr\right)dr \tag{S20}$$

The first integral term on the right side of eq S20 is the solution to the depletion region current for a planar (one-dimensional) semiconductor photoelectrode described by Shockley and co-workers.[2]

$$q\int_{w}^{r_0} U(r)dr = J_{dr,planar} \tag{S21}$$

$$J_{dr,cyl} = J_{dr,planar} - \frac{q}{r}\int_{w}^{r_0}\left(\int U(r)dr\right)dr \tag{S22}$$

Evaluation of the remaining integral term requires an explicit functional form for $U(r)$. Shockley and co-workers determined the following expression (eq S23),

$$U(r)=\frac{n_i}{\sqrt{\tau_n}\sqrt{\tau_p}}\frac{\sinh\left(\frac{qV}{2k_BT}\right)}{\cosh\left(\frac{q\left(\Psi(r)-\frac{V}{2}\right)}{k_BT}+\ln\sqrt{\frac{\tau_p}{\tau_n}}\right)+e^{\frac{-qV}{2k_BT}}\cosh\left(\frac{q(E_T-E_i)}{k_BT}+\ln\sqrt{\frac{\tau_p}{\tau_n}}\right)} \quad \text{(S23)}$$

where $\Psi(r)$ is the location-dependent electrostatic potential and E_T is the energy level of the trap states.

Assuming a linear potential drop across the depletion region in the radial direction, equivalent hole and electron lifetimes, and trap energy levels in the middle of the bandgap, eq S23 simplifies to eq S24.

$$U(r)=\frac{n_i}{\sqrt{\tau_n}\sqrt{\tau_p}}\frac{\sinh\left(\frac{qV}{2k_BT}\right)}{\cosh\left(\frac{q(V_{bi}-V)}{k_BT}\frac{r}{(r_0-w)}\right)+e^{\frac{-qV}{2k_BT}}} \quad \text{(S24)}$$

Substitution of eq S24 into eq S22 yields eq S25.

$$J_{dr,cyl}=J_{dr,planar}-\frac{qn_i\sinh\left(\frac{qV}{2k_BT}\right)}{r\sqrt{\tau_n}\sqrt{\tau_p}}\int_w^{r_0}\left(\int\frac{1}{\cosh\left(\frac{q(V_{bi}-V)}{k_BT}\frac{r}{(r_0-w)}\right)+e^{\frac{-qV}{2k_BT}}}dr\right)dr \quad \text{(S25)}$$

For simplicity, we choose to define this explicit integral as single term whose value is dependent upon the values of r_0 and w.

$$-Z(r_0,w)\equiv\int_w^{r_0}\left(\int\frac{1}{\cosh\left(\frac{q(V_{bi}-V)}{k_BT}\frac{r}{(r_0-w)}\right)+e^{\frac{-qV}{2k_BT}}}dr\right)dr \quad \text{(S26)}$$

Substitution of eq S26 into S25 gives eq S27.

$$J_{dr,cyl} = J_{dr,planar} + \frac{qn_i Z(r_0,w)\sinh\left(\frac{qV}{2k_BT}\right)}{r\sqrt{\tau_n}\sqrt{\tau_p}} \quad \text{(S27)}$$

When the bias is much larger than k_BT/q, the sinh term can be approximated by eq S28,

$$\sinh\left(\frac{qV}{2k_BT}\right) \approx \frac{1}{2}e^{\frac{qV}{2k_BT}} \quad \text{(S28)}$$

which gives eq S29.

$$J_{dr,cyl} = J_{dr,planar} + \frac{qn_i Z(r_0,w)}{2r\sqrt{\tau_n}\sqrt{\tau_p}}e^{\frac{qV}{2k_BT}} \quad \text{(S29)}$$

The function in eq S29 includes r in the second term. The explicit value of r determines whether the first or second term controls the value of $J_{dr,cyl}$. When the distribution of trap states is uniform (i.e. does not depend on r) and the quasi-Fermi levels are constant across the depletion region, there is a local maximum for $U(r)$ within the depletion region. If we define this position, $r_{dr,max}$, as the key descriptor for depletion region recombination, then eq S29 becomes eq S30.

$$J_{dr,cyl} = J_{dr,planar} + \frac{qn_i Z(r_0,w)}{2r_{dr,max}\sqrt{\tau_n}\sqrt{\tau_p}}e^{\frac{qV}{2k_BT}} \quad \text{(S30)}$$

When $\tau = \tau_n = \tau_p$ and $L_p = \sqrt{\tau_p D_p}$, eq S30 can be re-expressed in terms of L_p.

$$J_{dr,cyl} = J_{dr,planar} + \frac{qn_i Z(r_0,w)D_p}{2r_{dr,max}L_p^2}e^{\frac{qV}{2k_BT}} \quad \text{(S31)}$$

For small values of $r_{dr,max}$ and under illumination when depletion region recombination is limiting, the open-circuit photovoltage can be estimated from eq S32.

$$V_{oc} = \frac{2k_BT}{q}\ln\left(\frac{J_{ph}}{\frac{qn_i Z(r_0,w)D_p}{2r_{dr,max}L_p^2}}\right) \quad \text{(S32)}$$

S4. Description of the Simulation Device Grid.

The simulations utilized a device structure containing mesh with grid box sizes that were a function of both the proximity to a contact and the top of the nanowire. The meshing gradient with respect to the proximity to the contacts was used to ensure that electrostatic gradients could be calculated with sufficient accuracy and precision. The second meshing gradient with respect to the proximity of the top plane of the nanowire/structure was used to accurately model the absorption of short-wavelength photons. The accuracy of the grid structure in this respect was analyzed by determining the error in quantum efficiency at short (< 350 nm) wavelength light as a function of mesh size. Separately, a 5Å outer layer was used to model the effects of surface traps assuming Shockley-Read-Hall recombination.

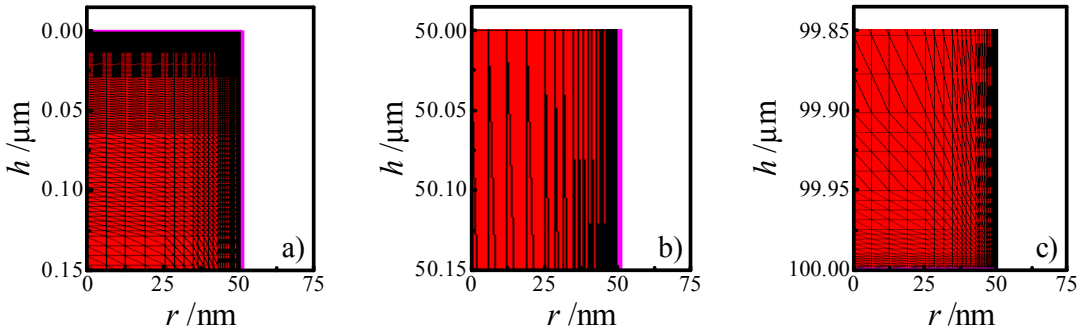

Figure S1. Pictorial representation of the computational mesh used for nanowire simulations in Sentaurus. (a) The top portion of the nanowire structure from the top edge to a depth of 0.15 µm; (b) the middle portion of the nanowire structure from the a depth of 50 to 50.15 µm; and (c) The bottom portion of the nanowire structure from the bottom edge to a height of 0.15 µm.

S5. Tables of Simulation Parameters

Table S1. Simulation Parameters for Figure 4

Parameter	Description	Value	Units
$q\,\Phi_b$	barrier height	1.0	eV
$\mathbf{E}_g$	bandgap	1.16964	eV
n_i	intrinsic carrier concentration	4.6×10^{9}	cm^{-3}
ε_{Si}	Si dielectric constant	11.7	
T	temperature	300	K
N_{CB}	effective density of states in conduction band	2.78×10^{19}	cm^{-3}
N_{VB}	effective density of states in valence band	3.14×10^{19}	cm^{-3}
N_D	dopant density	10^{16} - 3.162×10^{17}	cm^{-3}
τ_n	bulk electron lifetime	2.0568×10^{-6}	s
τ_p	bulk hole lifetime	2.0568×10^{-6}	s
$\tau_{n,s}$	surface electron lifetime	5×10^{-8}	s
$\tau_{p,s}$	surface hole lifetime	5×10^{-8}	s
$k_{Aug,n}$	Auger recombination coefficient for electrons	6.7×10^{-32}	$cm^6\ s^{-1}$
$k_{Aug,p}$	Auger recombination coefficient for holes	7.2×10^{-32}	$cm^6\ s^{-1}$
h	nanowire height	100	um
r	nanowire radius	50	nm
μ_n	electron mobility	1417	$cm^2\ V^{-1}\ s^{-1}$
μ_p	hole mobility	470.5	$cm^2\ V^{-1}\ s^{-1}$
$k_{et}[A]$	electron contact velocity	1×10^{2}	$cm\ s^{-1}$
$k_{ht}[A^-]$	hole contact velocity	1×10^{2}	$cm\ s^{-1}$
I_0	incident photon flux, 750 nm wavelength	1×10^{17}	photons $cm^{-2}\ s^{-1}$
α	Si absorptivity at 750 nm	1.5×10^{3}	cm^{-1}

Table S2. Simulation Parameters for Figure 5

Parameter	Description	Value	Units
$q\,\Phi_b$	barrier height	1.0	eV
$\mathbf{E}_g$	bandgap	1.16964	eV
n_i	intrinsic carrier concentration	4.6×10^{9}	cm^{-3}
ε_{Si}	Si dielectric constant	11.7	
T	temperature	300	K
N_{CB}	effective density of states in conduction band	2.78×10^{19}	cm^{-3}
N_{VB}	effective density of states in valence band	3.14×10^{19}	cm^{-3}
N_D	dopant density	2×10^{16}	cm^{-3}
τ_n	bulk electron lifetime	6.8221×10^{-7}	s
τ_p	bulk hole lifetime	2.0568×10^{-6}	s
$\tau_{n,s}$	surface electron lifetime	5×10^{-8}	s
$\tau_{p,s}$	surface hole lifetime	5×10^{-8}	s
$k_{Aug,n}$	Auger recombination coefficient for electrons	6.7×10^{-32}	$cm^6\ s^{-1}$
$k_{Aug,p}$	Auger recombination coefficient for holes	7.2×10^{-32}	$cm^6\ s^{-1}$
h	nanowire height	100	um
r	nanowire radius	50-300	nm
μ_n	electron mobility	1417	$cm^2\ V^{-1}\ s^{-1}$
μ_p	hole mobility	470.5	$cm^2\ V^{-1}\ s^{-1}$
$k_{et}[A]$	electron contact velocity	1×10^{2}	$cm\ s^{-1}$
$k_{ht}[A^-]$	hole contact velocity	1×10^{2}	$cm\ s^{-1}$
I_0	AM1.5 simulated solar spectrum	100	$mW\ cm^{-2}$

Table S3. Simulation Parameters for Figure 6

Parameter	Description	Value	Units
$q\Phi_b$	barrier height	1.0	eV
$\mathbf{E}_g$	bandgap	1.16964	eV
n_i	intrinsic carrier concentration	4.6×10^{9}	cm^{-3}
ε_{Si}	Si dielectric constant	11.7	
T	temperature	300	K
N_{CB}	effective density of states in conduction band	2.78×10^{19}	cm^{-3}
N_{VB}	effective density of states in valence band	3.14×10^{19}	cm^{-3}
N_D	dopant density	1×10^{18}	cm^{-3}
τ_n	bulk electron lifetime	2.06×10^{-12} - 2.06×10^{-6}	s
τ_p	bulk hole lifetime	2.06×10^{-12} - 2.06×10^{-6}	s
$\tau_{n,s}$	surface electron lifetime	5×10^{-8}	s
$\tau_{p,s}$	surface hole lifetime	5×10^{-8}	s
$k_{Aug,n}$	Auger recombination coefficient for electrons	6.7×10^{-32}	$cm^6\ s^{-1}$
$k_{Aug,p}$	Auger recombination coefficient for holes	7.2×10^{-32}	$cm^6\ s^{-1}$
h	nanowire height	100	um
r	nanowire radius	50	nm
μ_n	electron mobility	1.417×10^{-3} - 1.417×10^{5}	$cm^2\ V^{-1}\ s^{-1}$
μ_p	hole mobility	4.70×10^{-4} - 4.70×10^{4}	$cm^2\ V^{-1}\ s^{-1}$
$k_{et}[A]$	electron contact velocity	1×10^{2}	$cm\ s^{-1}$
$k_{ht}[A^-]$	hole contact velocity	1×10^{2}	$cm\ s^{-1}$
I_0	AM1.5 white light illumination	100	$mW\ cm^{-2}$

Table S4. Simulation Parameters for Figure 7a

Parameter	Description	Value	Units
$q\,\Phi_b$	barrier height	1.0	eV
$\mathbf{E}_g$	bandgap	1.16964	eV
n_i	intrinsic carrier concentration	4.6×10^{9}	cm^{-3}
ε_{Si}	Si dielectric constant	11.7	
T	temperature	300	K
N_{CB}	effective density of states in conduction band	2.78×10^{19}	cm^{-3}
N_{VB}	effective density of states in valence band	3.14×10^{19}	cm^{-3}
N_D	dopant density	1×10^{18}	cm^{-3}
τ_n	bulk electron lifetime	8.6×10^{-14} - 6.8×10^{-13}	s
τ_p	bulk hole lifetime	8.6×10^{-14} -6.8×10^{-13}	s
$\tau_{n,s}$	surface electron lifetime	5×10^{-13} - 5×10^{-8}	s
$\tau_{p,s}$	surface hole lifetime	5×10^{-13} - 5×10^{-8}	s
$k_{Aug,n}$	Auger recombination coefficient for electrons	6.7×10^{-32}	$cm^6\ s^{-1}$
$k_{Aug,p}$	Auger recombination coefficient for holes	7.2×10^{-32}	$cm^6\ s^{-1}$
h	nanowire height	100	um
r	nanowire radius	50 - 100	nm
μ_n	electron mobility	1417	$cm^2\ V^{-1}\ s^{-1}$
μ_p	hole mobility	470	$cm^2\ V^{-1}\ s^{-1}$
$k_{et}[A]$	electron contact velocity	1×10^{2}	$cm\ s^{-1}$
$k_{ht}[A^-]$	hole contact velocity	1×10^{2}	$cm\ s^{-1}$
I_0	AM1.5 white light illumination	100	$mW\ cm^{-2}$

Table S5. Simulation Parameters for Figure 7b

Parameter	Description	Value	Units
$q\,\Phi_b$	barrier height	1.0	eV
$\mathbf{E}_g$	bandgap	1.16964	eV
n_i	intrinsic carrier concentration	4.6×10^{9}	cm^{-3}
ε_{Si}	Si dielectric constant	11.7	
T	temperature	300	K
N_{CB}	effective density of states in conduction band	2.78×10^{19}	cm^{-3}
N_{VB}	effective density of states in valence band	3.14×10^{19}	cm^{-3}
N_D	dopant density	1×10^{18}	cm^{-3}
τ_n	bulk electron lifetime	2.0537×10^{-10} - 2.0537×10^{-6}	s
τ_p	bulk hole lifetime	2.0537×10^{-10} - 2.0537×10^{-6}	s
$\tau_{n,s}$	surface electron lifetime	5×10^{-8}	s
$\tau_{p,s}$	surface hole lifetime	5×10^{-8}	s
$k_{Aug,n}$	Auger recombination coefficient for electrons	6.7×10^{-32}	$cm^6\ s^{-1}$
$k_{Aug,p}$	Auger recombination coefficient for holes	7.2×10^{-32}	$cm^6\ s^{-1}$
h	nanowire height	100	um
r	nanowire radius	50 - 50000	nm
μ_n	electron mobility	1417	$cm^2\ V^{-1}\ s^{-1}$
μ_p	hole mobility	470	$cm^2\ V^{-1}\ s^{-1}$
$k_{et}[A]$	electron contact velocity	1×10^{2}	$cm\ s^{-1}$
$k_{ht}[A^-]$	hole contact velocity	1×10^{2}	$cm\ s^{-1}$
I_0	AM1.5 white light illumination	100	$mW\ cm^{-2}$

Table S6. Simulation Parameters for Figure 7c

Parameter	Description	Value	Units
$q\,\Phi_b$	barrier height	1.0 - 2.0	eV
$\mathbf{E}_g$	bandgap	2.26	eV
n_i	intrinsic carrier concentration	0.044	cm^{-3}
ε_{Si}	GaP dielectric constant	10.2	
T	temperature	300	K
N_{CB}	effective density of states in conduction band	1.78×10^{18}	cm^{-3}
N_{VB}	effective density of states in valence band	1.92×10^{19}	cm^{-3}
N_D	dopant density	1×10^{18}	cm^{-3}
τ_n	bulk electron lifetime	1.287×10^{-11} - 1.287×10^{-7}	s
τ_p	bulk hole lifetime	1.287×10^{-11} - 1.287×10^{-7}	s
$\tau_{n,s}$	surface electron lifetime	5×10^{-13} - 5×10^{-8}	s
$\tau_{p,s}$	surface hole lifetime	5×10^{-13} - 5×10^{-8}	s
$k_{Aug,n}$	Auger recombination coefficient for electrons	1×10^{-30}	$cm^6\ s^{-1}$
$k_{Aug,p}$	Auger recombination coefficient for holes	1×10^{-30}	$cm^6\ s^{-1}$
h	nanowire height	100	um
r	nanowire radius	50	nm
μ_n	electron mobility	110	$cm^2\ V^{-1}\ s^{-1}$
μ_p	hole mobility	75	$cm^2\ V^{-1}\ s^{-1}$
$k_{et}[A]$	electron contact velocity	1×10^2	$cm\ s^{-1}$
$k_{ht}[A^-]$	hole contact velocity	1×10^2	$cm\ s^{-1}$
I_0	AM1.5 white light illumination	100	$mW\ cm^{-2}$

Table S7. Simulation Parameters for Figure 7d

Parameter	Description	Value	Units
$q\,\Phi_b$	barrier height	1.0 - 2.0	eV
$\mathbf{E}_g$	bandgap	2.26	eV
n_i	intrinsic carrier concentration	0.044	cm^{-3}
ε_{Si}	GaP dielectric constant	10.2	
T	temperature	300	K
N_{CB}	effective density of states in conduction band	1.78×10^{18}	cm^{-3}
N_{VB}	effective density of states in valence band	1.92×10^{19}	cm^{-3}
N_D	dopant density	1×10^{18}	cm^{-3}
τ_n	bulk electron lifetime	5.148×10^{-11} - 1.287×10^{-9}	s
τ_p	bulk hole lifetime	5.148×10^{-11} - 1.287×10^{-9}	s
$\tau_{n,s}$	surface electron lifetime	5×10^{-8}	s
$\tau_{p,s}$	surface hole lifetime	5×10^{-8}	s
$k_{Aug,n}$	Auger recombination coefficient for electrons	1×10^{-30}	$cm^6\ s^{-1}$
$k_{Aug,p}$	Auger recombination coefficient for holes	1×10^{-30}	$cm^6\ s^{-1}$
h	nanowire height	100	um
r	nanowire radius	50	nm
μ_n	electron mobility	110	$cm^2\ V^{-1}\ s^{-1}$
μ_p	hole mobility	75	$cm^2\ V^{-1}\ s^{-1}$
$k_{et}[A]$	electron contact velocity	1×10^2	$cm\ s^{-1}$
$k_{ht}[A^-]$	hole contact velocity	1×10^2	$cm\ s^{-1}$
I_0	AM1.5 white light illumination	100	$mW\ cm^{-2}$

Table S8. Simulation Parameters for Figure 8a,b

Parameter	Description	Value	Units
$q\,\Phi_b$	barrier height	1.0	eV
$\mathbf{E}_g$	bandgap	1.16964	eV
n_i	intrinsic carrier concentration	4.6×10^{9}	cm^{-3}
ε_{Si}	Si dielectric constant	11.7	
T	temperature	300	K
N_{CB}	effective density of states in conduction band	2.78×10^{19}	cm^{-3}
N_{VB}	effective density of states in valence band	3.14×10^{19}	cm^{-3}
N_D	dopant density	1×10^{18}	cm^{-3}
τ_n	bulk electron lifetime	8.2149×10^{-10}	s
τ_p	bulk hole lifetime	8.2149×10^{-10}	s
$\tau_{n,s}$	surface electron lifetime	5×10^{-13} - 5×10^{-8}	s
$\tau_{p,s}$	surface hole lifetime	5×10^{-13} - 5×10^{-8}	s
$k_{Aug,n}$	Auger recombination coefficient for electrons	6.7×10^{-32}	$cm^6\ s^{-1}$
$k_{Aug,p}$	Auger recombination coefficient for holes	7.2×10^{-32}	$cm^6\ s^{-1}$
h	nanowire height	100	um
r	nanowire radius	50	nm
μ_n	electron mobility	1417	$cm^2\ V^{-1}\ s^{-1}$
μ_p	hole mobility	470	$cm^2\ V^{-1}\ s^{-1}$
$k_{et}[A]$	electron contact velocity	1×10^{2}	$cm\ s^{-1}$
$k_{ht}[A^-]$	hole contact velocity	1×10^{2}	$cm\ s^{-1}$
I_0	AM1.5 white light illumination	100	$mW\ cm^{-2}$

Table S9. Simulation Parameters for Figure 8c

Parameter	Description	Value	Units
$q\Phi_b$	barrier height	1.0 - 2.0	eV
$\mathbf{E}_g$	bandgap	2.26	eV
n_i	intrinsic carrier concentration	0.66	cm^{-3}
ε_{Si}	GaP dielectric constant	10.2	
T	temperature	300	K
N_{CB}	effective density of states in conduction band	1.78×10^{18}	cm^{-3}
N_{VB}	effective density of states in valence band	1.92×10^{19}	cm^{-3}
N_D	dopant density	1×10^{18}	cm^{-3}
τ_n	bulk electron lifetime	5.148×10^{-11}	s
τ_p	bulk hole lifetime	5.148×10^{-11}	s
$\tau_{n,s}$	surface electron lifetime	5×10^{-13} - 5×10^{-8}	s
$\tau_{p,s}$	surface hole lifetime	5×10^{-13} - 5×10^{-8}	s
$k_{Aug,n}$	Auger recombination coefficient for electrons	1×10^{-30}	$cm^6\ s^{-1}$
$k_{Aug,p}$	Auger recombination coefficient for holes	1×10^{-30}	$cm^6\ s^{-1}$
h	nanowire height	100	um
r	nanowire radius	50	nm
μ_n	electron mobility	110	$cm^2\ V^{-1}\ s^{-1}$
μ_p	hole mobility	75	$cm^2\ V^{-1}\ s^{-1}$
$k_{et}[A]$	electron contact velocity	1×10^2	$cm\ s^{-1}$
$k_{ht}[A^-]$	hole contact velocity	1×10^2	$cm\ s^{-1}$
I_0	AM1.5 white light illumination	100	$mW\ cm^{-2}$

Table S10. Simulation Parameters for Figure 9

Table S10. Simulation Parameters for Figure 9.

Parameter	Description	Value	Units
$q\,\Phi_b$	barrier height	1.0,[a] N/A[b]	eV
$\mathbf{E}_g$	bandgap	1.16964	eV
n_i	intrinsic carrier concentration	4.6×10^{9}	cm^{-3}
ε_{Si}	Si dielectric constant	11.7	
T	temperature	300	K
N_{CB}	effective density of states in conduction band	2.78×10^{19}	cm^{-3}
N_{VB}	effective density of states in valence band	3.14×10^{19}	cm^{-3}
N_D	dopant density	1×10^{12}	cm^{-3}
$N_{Contacts}$	contact maximum dopant density	1×10^{19}	cm^{-3}
τ_n	bulk electron lifetime	8.2149×10^{-10}	s
τ_p	bulk hole lifetime	8.2149×10^{-10}	s
$\tau_{n,s}$	surface electron lifetime	5×10^{-8}	s
$\tau_{p,s}$	surface hole lifetime	5×10^{-8}	s
$k_{Aug,n}$	Auger recombination coefficient for electrons	6.7×10^{-32}	$cm^6\ s^{-1}$
$k_{Aug,p}$	Auger recombination coefficient for holes	7.2×10^{-32}	$cm^6\ s^{-1}$
h	nanowire height	30	μm
r	nanowire radius	50	nm
μ_n	electron mobility	1417	$cm^2\ V^{-1}\ s^{-1}$
μ_p	hole mobility	470	$cm^2\ V^{-1}\ s^{-1}$
v_n	electron contact velocity	1×10^{7}	$cm\ s^{-1}$
v_p	hole contact velocity	1×10^{7}	$cm\ s^{-1}$
I_0	AM1.5 white light illumination	10^2 - 10^5	$mW\ cm^{-2}$
α	Si spectral absorptivity	1.1 - 2.4×10^{6}	cm^{-1}

a. Barrier height for conformal junction in Figure 9a

b. No conformal junction was used in Figure 9c

S6. References

1. Carslaw, H. S. Introduction to the Mathematical Theory of the Conduction of Heat in Solids, 2nd ed., Macmillan and Co., Ltd., **1921**

2. Sah, C.; Noyce, R. N.; Shockley, W. *Proc. IRE*, **1957**, *45*, 1228-1243